in cell proliferation, organ growth, and apoptosis. In our research, it is found in the promoters of INS, RPS6KA2 (*module 1*), IRS1, PIK3R1, PIK3CA (*module 2*), TNF (*module 3*), and TSC2 (*module 4*). Akhtar et al. (2012) suggest that PLAG1 is overexpressed in cancer cells when it binds to IGF2 promoter. Because of the close proximity of the IRS1 and IGF genes, PLAG1 may also regulate IRS1 as it was identified in our research.

Pre-core *modules 1* (MAPK signaling) and *2* (Insulin signaling) share SP1, MZF1, and PLAG1 transcription factors. Apart from it, *module 2* has FOXF2 (forkhead box F2) and TBP (TATA-binding protein). FOXF2 and TBP are already known in the context of *co*-regulation with MTOR, RDS1, (adenine-repressible gene) and TFAP2A (transcription factor AP-2 alpha) (Westergren, 2010).

FOXF2 is classified as TF, which regulates the mTOR pathway. The increased amount of FOXF2 inhibits the activity of IRS1 (insulin receptor substrate 1), leading to inhibition of the whole mTOR pathway via a negative-feedback loop (Westergren, 2010). FOXF2 interacts with another transcription factor TBP (TATA-binding protein), and in our research, both of them were found in close proximity to IRS1. TBP additionally interacts with SP1 and E2F1 transcription factors found in the *intersection zone* of mostly interconnected genes in our study (**Supporting Figure 1A**). In *module 2*, TBP is regulated by PI3K genes, and in the mTOR *core*, TBP is regulated by the MTOR gene, thus, playing a vital role in recruiting Polymerase I and modulating activity of Polymerase III (Cianfrocco et al., 2013).

In consideration of the locations of TFAP2A binding motifs, it is noteworthy that TFAP2A can regulate the mTOR pathway and, in particular, its *core* path. A TFAP2A binding motif was found in the promoters of IRS1 and PIK3R2 genes of an insulin signaling pathway (*module 2*), a PTEN gene, which is an inhibitor of the mTOR pathway thought the PIP3 (*module 2*) and RRAGD genes (*module 5*). TFAP2A is thus involved in processes of organ development and negative cell proliferation at the same time. One of the probable scenarios concerning TFAP2A is that by inhibition of IRS1, PIK3R2 (*module 2*), and RRAGD (*module 5*) genes, TFAP2A stimulates the PTEN transcription immobilizing mTOR pathway and negative feedback loop may exist between insulin-signaling *module 2* and amino-acid balance *module 5*. Surprisingly, a TF characteristic for yeast RDS1 (an adenine-repressible gene), responsible for the regulation of transcription from RNA polymerase II, is identified in the human data set. RDS1 binding motif is found in the promoters of IRS1, AKT1 (threonine-protein kinase) genes of pre-core *module 2*, and the RRAGC (Ras-related GTP binding C) gene of post-core *module 5*. It is difficult to assess RDS1 functions in an mTOR pathway due to the fact that it is only been found in yeast to date. However, in yeast organisms, it is responsible for transcription regulation and response to xenobiotic stimulus. In human organisms, its function may be very similar to the function in yeast, and human ortholog might be identified in the future.

RDS1 can influence the mTOR pathway from two sides: first, being regulated by growth factors and hormones (IRS1 and AKT1 in *module 2*) and, second, being regulated by the availability of amino acids or generally intracellular xenobiotics (RRAGC *in module 5*). The above-described finding on RDS1 activity indicates the existence of crosstalk between module 2 (insulin signaling) and module 5 (amino-acid balance within a cell) transcription regulation and existence of a negative feedback loop between them. This is a biologically reasonable finding as insulin-control amino-acid metabolism is tightly related to amino-acid-uptake balance.

MODULE FOUR REGULATES HYPOXIA

ARNT (aryl-hydrocarbon receptor nuclear translocator 3, HIF-1β) is one that regulates gene expression in hypoxia *module 4*. It encodes a protein that is crucial for complex formation with the ligand-bound aryl hydrocarbon receptor (AHR) and proper functioning of this receptor. Current knowledge indicates that the HIF1- and/or HIF2-mediated hypoxia responses can be oncogenic as well as tumor suppressive (Pawlis and Hu, 2013). ARNT induces activation of REDD1 (DDIT4) by creating a dimer with HIF1, thereby inhibiting TORC1 and affecting the TSC2-depending mechanism (Kapahi et al., 2010). ARNT interacts with ESR1, co-activating its transcription (Endler et al., 2004), and with SP1, creating a reconstituent complex (Mulero-Navarro et al., 2006) with it. SP1 itself is able to bind the Ah receptor and down-regulates its expression in leukemia cells (Mulero-Navarro et al., 2006).

CORE MODULE OF mTOR

In the core of mTOR pathway KLF4 (Kruppel-like factor 4) inhibits the MTOR gene and has an anti-proliferative effect on the whole mTOR pathway (Wang et al., 2012), thereby promoting self-renewal and precluding differentiation.

On the contrary, MEF2A (myocyte specific enhancer factor) positively regulates genes of the mTOR/S6K pathway, so it belongs both to the mTOR *core* and *module 7* (VEGF pathway) (Pereira et al., 2009; Yin et al., 2012), promoting cell growth and differentiation. However, the MEF2 family is also responsible for cardiac hypertrophy and failure (Pereira et al., 2009), and its overexpression leads to cardiac dysfunction.

MODULE SEVEN OF VEGF PATHWAY

Module 7 is associated with VEGF (vascular endothelial growth factor) pathway-advancing cell growth, organ development, and protein formation. This transcriptional module possesses four transcription factors, namely, SP1, ESR1, E2F1, and EGR1, with three first TFs tightly associated with the activities of the mTOR pathway.

EGR1 (early-growth-response protein 1), which is *module 7* specific TF, directs cell differentiation. It was discovered that its level in a prostate cancer was raised, showing a pro-oncogenic character; however, in other tumor types (skin tumor, fibrosarcoma, and glioblastoma), EGR1 exhibits features of a tumor suppressor by activating p53 and PTEN to halt the transcription of other genes in the mTOR pathway (Zheng et al., 2009). Moreover, it was discovered that the knockdown of EGR1 affects VEGFA, thereby affecting the VEGF pathway and mitogenesis (Abdel-Malak et al., 2009).

An E2F group affects activation of RPS6KB1 (S6K) and stimulates phosphorylation of S6K and 4EBP in the presence of Leucine. E2F1 integrates cell division (as well as cell growth) and

induces an apoptotic response (Real et al., 2011). In tumor cells, it can activate EGR1 to endorse cell survival. Moreover, in tumor cells, by up-regulating the production of EGR1, epidermal growth factor (EGFR), platelet-derived growth factor (PDGFRA), and insulin-like growth factor II (IGF2BP2), E2F1 can activate the phosphoinositide-3-kinase/Akt (PIK3CA/AKT) pathway in a way to inhibit drug-induced apoptosis (Zheng et al., 2009).

DISCUSSION

Transcription factors selected (24 genes) from the results analysis where those identified by main and supportive motifs discovery tools used in our study (**Supporting Figure 1**). Other transcription factors that less frequently appear can be seen in the process-module-assigned fashion in **Supporting Figures 1A,B** for human and mouse, respectively. Transcription factors (24) are classified into two groups: first, those expressed in the specific module of mTOR and second, those commonly identified in various modules.

The first group of TFs includes ESR1, ELK1 (MAPK signaling, *module 1*), FOXF2 (Insulin signaling, *module 2*), KLF4 (*mTOR core*), ARNT (Hypoxia, *module 4*), E2F1, and EGR1 (VEGF signaling, *module 7*). The second group includes SP1, MZF1, PLAG1, TFAP1A, TBP, and RDS1. Among member of the second group, MZF1, PLAG1, TFAP1A, and RDS are newly identified. Other transcription factors identified in the promoters of genes in our analysis are EGR2, EGR3, YY1, SREBF1, SREBF2, ELF1, and ARID3A. They are less frequently share by the promoters in our dataset but they are well-known to be involved in the mTOR pathway regulation (YY1, SREBFs).

One-third (21) of the human transcription factors were found to be conserved in the case of a mouse. Among them most confident are SP1, TFAP2A, MZF1, EGR3, KLF4, USF1, KLF9, and ARNT (**Supporting Figure 1B**). They are transcription factors having multiple copies in gene promoters and/or shared by many genes within the dataset. Cross-species-conserved TFs identified corroborate the consistency of our methodology. However, a part of frequently appearing mouse TFs, such as HSF1, CDC5L, HES6, and FOXL1, were not identified in orthologous human promoters. This might be regarding to the difference in the transcription regulation between two species.

The results described in the paper indicate that the proper selection of online motif-discovery tools without parameters tuning is feasible to bring accurate results for the discovery transcription regulation on medium size data. However the aim to reduce false positives might result in the omitting low sensitivity-degenerate motifs (Polouliakh et al., 2005). Creation of sophisticated analytic workflow might be warranted to cope with large-scale sequence data for *de novo* motif discovery.

AUTHOR CONTRIBUTIONS

Agnieszka Jablonksa analyzed data and wrote the manuscript. Natalia Polouliakh discussed the research and wrote the manuscript.

ACKNOWLEDGMENTS

We greatly appreciate the scientific support and comments of Prof. Hiroaki Kitano (Sony Computer Science Laboratories Inc., Japan), Prof. Huaiyu Mi (University of Southern California, USA) and Dr. Yukiko Matsuoka (Systems Biology Institute, Japan).

SUPPLEMENTARY MATERIAL

The Supplementary Material for this article can be found online at: http://www.frontiersin.org/journal/10.3389/fcell.2014.00023/abstract

Supporting Figure 1 | Transcription-factor (TF) binding motifs in the mTOR pathway identified in human (A) and mouse (B) orthologous datasets. The intensity of the blue color reflects frequency of motif occurrence per gene. The colors above transcription-factor names point to those supportive programs (Cscan, LocaMo, TransFind, and TRAP), which also identified a motif after it was detected by the five main programs (MEME_Chip, PASTAA, Pscan, TFM-Explorer, and XXmotif). Transcription factors were sorted according to the sum of occurrences in the whole data set. The red horizontal line in the human-case results highlights 24 genes with average number of motifs per gene higher than 26 (Gene threshold, Gene_TH), and the vertical red line shows the top-24 transcription factors (TF_TH) identified as the most significant in our study. Sub-table **(B)** shows mouse transcription factors and genes in the same order with the human ones and extended red lines from human data in order to depict similarities between two species. Sub-table **(C)** includes description of transcription factors and estimated positions of their motifs in human promoters based on the results of the five main programs (MEME_Chip, PASTAA, Pscan, TFM-Explorer, and XXmotif) and asterisks point to human-mouse orthologous TFs.

REFERENCES

Abdel-Malak, N. A., Mofarrahi, M., Mayaki, D., Khachigian, L. M., and Hussain, S. N. A. (2009). Early growth response-1 regulates angiopoietin-1-induced endothelial cell proliferation, migration, and differentiation. *Arterioscler. Thromb. Vasc. Biol.* 29, 209–216. doi: 10.1161/ATVBAHA.108.181073

Akhtar, M., Holmgren, C., Göndör, A., Vesterlund, M., Kanduri, C., Larsson, C., et al. (2012). Cell type and context-specific function of PLAG1 for IGF2 P3 promoter activity. *Int. J. Oncol.* 41, 1959–1966. doi: 10.3892/ijo.2012.1641

Alam, H., Maizels, E. T., Park, Y., Ghaey, S., Feiger, Z. J., Chandel, N. S., et al. (2004). Follicle-stimulating Hormone Activation of Hypoxia-inducible Factor-1 by the Phosphatidylinositol 3-Kinase/AKT/Ras Homolog Enriched in Brain (Rheb)/Mammalian Target of Rapamycin. *J. Biol. Chem.* 279, 19431–19440. doi: 10.1074/jbc.M401235200

Ao, W., Gaudet, J., Kent, W. J., Muttumu, S., and Mango, S. E. (2004). Environmentally induced foregut remodeling by PHA-4/FoxA and DAF-12/NHR. *Science* 305, 1743–1746. doi: 10.1126/science.1102216

Bailey, T. L., Boden, M., Buske, F. A., Frith, M., Grant, C. E., Clementi, L., et al. (2009). MEME SUITE: tools for motif discovery and searching. *Nucleic Acids Res.* 37, W202–W208. doi: 10.1093/nar/gkp335

Blagosklonny, M. V. (2006). Aging and Immortality Quasi-programmed Senescence and Its Pharmacologic Inhibition. *Cell Cycle* 5, 2087–2102. doi: 10.4161/cc.5.18.3288

Broos, S., Hulpiau, P., Galle, J., Hooghe, B., Roy, V. F., and Bleser, P. D. (2011). ConTra v2: a tool to identify transcription factor binding sites across species, update 2011. *Nucleic Acids Res.* 39, W74–W78. doi: 10.1093/nar/gkr355

Brown, E. J., Albers, M. W., Shin, T. B., Ichikawa, K., Keith, C. T., Lane, W. S., et al. (1994). A mammalian protein targeted by G1-arresting rapamycin-receptor complex. *Nature* 369, 756–758. doi: 10.1038/369756a0

Carlson, J. M., Chakravarty, A., DeZiel, C. E., and Gross, R. H. (2007). SCOPE: a web server for practical de novo motif discovery. *Nucleic Acids Res.* 35, W259–W264. doi: 10.1093/nar/gkm310

Caron, E., Ghosh, S., Matsuoka, Y., Ashton-Beaucage, D., Therrien, M., Lemieux, L., et al. (2010). A comprehensive map of the mTOR signaling network. *Mol. Syst. Biol.* 6, 453. doi: 10.1038/msb.2010.108

Chaivorapol, C., Melton, C., Wei, G., Yeh, R. F., Ramalho-Santos, M., Blelloch, R., et al. (2008). CompMoby: comparative MobyDick for detection of cis-regulatory motifs. *BMC Bioinformatics* 9:455. doi: 10.1186/1471-2105-9-455

Cianfrocco, M. A., Kassavetis, G. A., Grob, P., Fang, J., Juven-Gershon, T., Kadonaga, J. T., et al. (2013). Human TFIID binds to core promoter DNA in a reorganized structural state. *Cell* 152, 120–131. doi: 10.1016/j.cell.2012.12.005

Defrance, M., Touzet, H. (2006). Predicting transcription factor binding sites using local over-representation and comparative genomics *BMC Bioinformatics* 7:396. doi: 10.1186/1471-2105-7-396

Deprost, D., Yao, L., Sormani, R., Moreau, M., Leterreux, G., Nicola, M., et al. (2007). The Arabidopsis TOR kinase links plant growth, yield, stress resistance and mRNA translation. *EMBO Rep.* 8, 864–870. doi: 10.1038/sj.embor.7401043

Dinh, H., Rajasekaran, S., and Kundeti, V. K. (2011). PMS5: an efficient exact algorithm for the (l,d)-motif finding problem. *BMC Bioinformatics* 12:410. doi: 10.1186/1471-2105-12-410

Endler, A., Chen, L., Zhang, J., Xu, G. T., and Shibasaki, F. (2004). Binding of the ER_ and ARNT1 AF2 domains to exon 21 of the SRC1 isoform SRC1e is essential for estrogen- and dioxin-related transcription. *J. Cell Sci.* 125, 2004–2016 doi: 10.1242/jcs.097246

Favorov, A. V., Gelfand, M. S., Gerasimova, A. V., Ravcheev, D. A., Mironov, A. A., and Makeev, V. J. (2005). A Gibbs sampler for identification of symmetrically structured, spaced DNA motifs with improved estimation of the signal length. *Bioinformatics* 21:10. doi: 10.1093/bioinformatics/bti336

Fu, Y., Frith, M. C., Haverty, P. M., and Weng, Z. (2004). MotifViz: an analysis and visualization tool for motif discovery. *Nucleic Acids Res.* 32, W420–W423. doi: 10.1093/nar/gkh426

Funahashi, A., Tanimura, N., Morohashi, M., and Kitano, H. (2003). CellDesigner: a process diagram editor for gene-regulatory and biochemical networks. *Biosilico* 1, 159–162. doi: 10.1016/S1478-5382(03)02370-9

Ghosh, S., Matsuoka, Y., Asai, Y., Hsin, K. Y., and Kitano, H. (2011). Software for systems biology: from tools to integrated platforms. *Nat. Rev. Genet.* 12, 821–832. doi: 10.1038/nrg3096

Hall, M. N. (2008). mTOR-what does it do? *Transplant. Proc.* 40, S5–S8. doi: 10.1016/j.transproceed.2008.10.009

Hay, N., and Sonenberg, N. (2004). Upstream and downstream of mTOR. *Genes Dev.* 18, 1926–1945. doi: 10.1101/gad.1212704

Heinemeyer, T., Wingender, E., Reuter, I., Hermjakob, H., Kel, A. E., Kel, O. V., et al. (1998). Databases on transcriptional regulation: TRANSFAC, TRRD and COMPEL. *Nucleic Acids Res.* 26, 362–367. doi: 10.1093/nar/26.1.362

Heitman, J., Movva, N. R., and Hall, M. N. (1991). Targets for cell cycle arrest by the immunosuppressant rapamycin in yeast. *Science* 253, 905–909. doi: 10.1126/science.1715094

Inoki, K., and Guan, K. L. (2006). Complexity of the TOR signaling network. *Trends Cell Biol.* 16, 206–212. doi: 10.1016/j.tcb.2006.02.002

Inoki, K., Ouyang, H., Li, Y., and Guan, K. L. (2005). Signaling by target of rapamycin proteins in cell growth control. *Microbiol. Mol. Biol. Rev.* 69, 79–100. doi: 10.1128/MMBR.69.1.79-100.2005

Johnson, S. C., Rabinovitch, P. S., and Kaeberlein, M. (2013). mTOR is a key modulator of ageing and age-related diseases. *Nature* 493, 338. doi: 10.1038/nature11861

Kapahi, P., Chen, D., Rogers, A. N., Katewa, S. D., Li, P. W., Thomas, E. L., et al. (2010). With TOR, less is more: a key role for the conserved nutrient-sensing TOR pathway in aging. *Cell Metab.* 11, 453–65. doi: 10.1016/j.cmet.2010.05.001

Kielbasa, S. M., Klein, H., Roider, H. G., Vingron, M., and Blüthgen, N. (2010). TransFind - predicting transcriptional regulators for gene sets. *Nucleic Acids Res.* 38, W275–W280. doi: 10.1093/nar/gkq438

Kobayashi, T., Minowa, O., Sugitani, Y., Takai, S., Mitani, H., Kobayashi, E., et al. (2001). A germ-line Tsc1 mutation causes tumor development and embryonic lethality that are similar, but not identical to, those caused by Tsc2 mutation in mice. *Proc. Natl. Acad. Sci. U.S.A.* 98, 8762–8769. doi: 10.1073/pnas.151033798

Laplante, M., and Sabatini, D. M. (2009). mTOR signaling at a glance. *J. Cell Sci.* 122, 3589–3594. doi: 10.1242/jcs.051011

Lee, C., and Huang, C. H. (2013). LASAGNA-Search: an integrated web tool for transcription factor binding site search and visualization. *BioTechniques* 54, 141–153. doi: 10.2144/000113999

Li, N., Zhong, M., and Song, M. (2012). Expression of phosphorylated mTOR and its regulatory protein is related to biological behaviors of ameloblastoma. *Int. J. Clin. Exp. Pathol.* 5, 660–667.

Liu, X., Brutlag, D. L., and Liu, J. S. (2001). Bioprospector: discovering conserved dna motifs in upstream regulatory regions of co-expressed genes. *Pac. Symp. Biocomput.* 6, 127–138.

Liu, X. S., Brutlag, D. L., and Liu, J. S. (2002). An algorithm for finding protein-DNA binding sites with applications to chromatin-immunoprecipitation microarray experiments. *Nat. Biotechnol.* 8, 835–839. doi: 10.1038/nbt717

Liu, Y., Liu, X. S., Wei, L., Altman, R. B., and Batzoglou, S. (2004). Eukaryotic regulatory element conservation analysis and identification using comparative genomics. *Genome Res.* 14, 451–458 doi: 10.1101/gr.1327604

Loots, G. G., and Ovcharenko, I. (2004). rVISTA 2.0: evolutionary analysis of transcription factor binding sites. *Nucleic Acids Res.* 32, W217–W221. doi: 10.1093/nar/gkh383

Lorberg, A., and Hall, M. N. (2004). TOR: the first 10 years. *Curr. Top Microbiol. Immunol.* 279, 1–18. doi: 10.1007/978-3-642-18930-2_1

Luehr, S., Hartmann, H., and Söding, J. (2012). The XXmotif web server for exhaustive, weight matrix-based motif discovery in nucleotide sequences. *Nucleic Acids Res.* 40, W104–W109. doi: 10.1093/nar/gks602

Mulero-Navarro, S., Carvajal-Gonzalez, J. M., Herranz, M., Ballestar, E., Fraga, M. F., Ropero, S., et al. (2006). The dioxin receptor is silenced by promoter hypermethylation in human acute lymphoblastic leukemia through inhibition of Sp1 binding. *Carcinogenesis* 27, 1099–1104. doi: 10.1093/carcin/bgi344

Murakami, M., Ichisaka, T., Maeda, M., Oshiro, N., Hara, K., Edenhofer, F., et al. (2004). mTOR is essential for growth and proliferation in early mouse embryos and embryonic stem cells. *Mol. Cell. Biol.* 24, 6710–6718. doi: 10.1128/MCB.24.15.6710-6718.2004

Néron, B., Ménager, H., Maufrais, C., Joly, N., Maupetit, J., Letort, S., et al. (2009). Mobyle: a new full web bioinformatics framework. *Bioinformatics* 25, 3005–3011. doi: 10.1093/bioinformatics/btp493

O'Neill, L. A. J., and Hardie, D. G. (2013). Metabolism of inflammation limited by AMPK and pseudo-starvation. *Nature* 493, 346–355.

Pawlis, M. R., and Hu, C. J. (2013). Enhanceosomes as integrators of hypoxia inducible factor (HIF) and other transcription factors in the hypoxic transcriptional response. *Cell. Signal.* 25, 1895–903. doi: 10.1016/j.cellsig.2013.05.018

Pereira, A. H., Clemente, C. F., Cardoso, A. C., Theizen, T. H., Rocco, S. A., Judice, C. C., et al. (2009). MEF2C silencing attenuates load-induced left ventricular hypertrophy by modulating mTOR/S6K pathway in mice. *PLoS ONE* 4:e8472. doi: 10.1371/journal.pone.0008472

Machanick, P, and Bailey, T. L. (2011). MEME-ChIP: motif analysis of large DNA datasets. *Bioinformatics* 27, 1696–1697. doi: 10.1093/bioinformatics/btr189

Polouliakh, N., Konno, M., Horton, P., and Nakai, K. (2005). Parameter lanscape analysis for common motif discovery programs. *Lect. Notes Comput. Sci.* 3318, 79–87. doi: 10.1007/978-3-540-32280-1_8

Polouliakh, N., Natsume, T., Harada, H., Fujibuchi, W., and Horton, P. (2006). Comparative genomic analysis of transcription regulation elements involved in human map kinase G-protein coupling pathway. *J. Bioinform. Comput. Biol.* 4, 469–482. doi: 10.1142/S0219720006001849

Polouliakh, N., Nock, R., Nielsen, F., and Kitano, H. (2009) G-Protein coupled receptor signaling architecture of mammalian immune cells. *PLoS ONE* 4:e4189. doi: 10.1371/journal.pone.0004189

Poluliakh, N., Takagi, T., and Nakai, K. (2003). MELINA: motif extraction from promoter regions of potentially co-regulated genes. *Bioinformatics* 19, 423–424. doi: 10.1093/bioinformatics/btf872

Real, S., Meo-Evoli, N., Espada, L., and Tauler, A. (2011). E2F1 regulates cellular growth by mTORC1 signaling. *PLoS ONE* 6:e16163. doi: 10.1371/journal.pone.0016163

Roider, H. G., Kanhere, A., Manke, T., and Vingron, M. (2007). Predicting transcription factor affinities to DNA from a biophysical model. *Bioinformatics* 23, 134–141. doi: 10.1093/bioinformatics/btl565

Roider, H. G., Manke, T., O'Keeffe, S., Vingron, M., and Haas, S. A. (2009). PASTAA: identifying transcription factors associated with sets of co-regulated genes. *Bioinformatics* 25, 435–442. doi: 10.1093/bioinformatics/btn627

Romer, K. A., Kayombya, G. R., and Fraenkel, E. (2007). WebMOTIFS: automated discovery, filtering and scoring of DNA sequence motifs using multiple programs and Bayesian approaches. *Nucleic Acids Res.* 35, W217–W220. doi: 10.1093/nar/gkm376

Sabatini, D. M., Erdjument-Bromage, H., Lui, M., Tempst, P., and Snyder, S. H. (1994). RAFT1: a mammalian protein that binds to FKBP12 in a rapamycin-dependent fashion and is homologous to yeast TORs. *Cell* 78, 35–43. doi: 10.1016/0092-8674(94)90570-3

Sandelin, A., Wasserman, W. W., and Lenhard, B. (2004). ConSite: web-based prediction of regulatory elements using cross-species comparison. *Nucleic Acids Res.* 32, W249–W252. doi: 10.1093/nar/gkh372

Schmelzle, T., and Hall, M. N. (2000). TOR, a central controller of cell growth. *Cell* 103, 253–262. doi: 10.1016/S0092-8674(00)00117-3

Serizawa, S., Miyamichi, K., Nakatani, H., Suzuki, M., Saito, M., Yoshihara, Y., et al. (2003). Negative feedback regulation ensures the one receptor - one olfactory neuron rule in mouse. *Science* 19, 2088–2094 doi: 10.1126/science.1089122

Siddharthan, R., Siggia, E. D., and van Nimwegen, E. (2005). PhyloGibbs: a Gibbs sampling motif finder that incorporates phylogeny. *PLoS Comput. Biol.* 1:e67. doi: 10.1371/journal.pcbi.0010067

Sinha, S., and Tompa, M. (2003). YMF: a program for discovery of novel transcription factor binding sites by statistical overrepresentation. *Nucleic Acids Res.* 31, 3586–3588. doi: 10.1093/nar/gkg618

Stanfel, M. N., Shamieh, L. S., Kaeberlein, M., and Kennedy, B. K. (2009). The TOR pathway comes of age. *Biochim. Biophys. Acta* 1790, 1067–1074. doi: 10.1016/j.bbagen.2009.06.007

Thompson, W., Rouchka, E. C., and Lawrence, C. E. (2003). Gibbs Recursive Sampler: finding transcription factor binding sites. *Nucleic Acids Res.* 31, 3580–3585. doi: 10.1093/nar/gkg608

Uht, R. M., Amos, S., Martin, P. M., Riggan, A. E., and Hussaini, I. M. (2007). The protein kinase C-g isoform induces proliferation in glioblastoma cell lines through an ERK/Elk-1 pathway. *Oncogene* 30, 2885–2893. doi: 10.1038/sj.onc.1210090

Vandenbon, A., Kumagai, Y., Teraguch, S., Amada, K. M., Akira, S., Daron, M., et al. (2013). A Parzen window-based approach for the detection of locally enriched transcription factor binding sites. *BMC Bioinformatics* 14:26. doi: 10.1186/1471-2105-14-26

Wang, Y., Zhao, B., Zhang, Y., Tang, Z., Shen, Q., Zhang, Y., et al. (2012). Krüppel-like factor 4 is induced by rapamycin and mediates the anti-proliferative rapamycin in rat carotid arteries. *Br. J. Pharmacol.* 165, 2378–2388. doi: 10.1111/j.1476-5381.2011.01734.x

Westergren, R. (2010). *Foxf2 and Foxc2, Two Transcription Factors that Regulate Adipocyte Metabolism.* Gothenburg: Intellecta Infolog.

Wijaya, E., Yiu, S. M., Son, N. T., Kanagasabai, R., and Sung, W. K. (2008). MotifVoter: a novel ensemble method for fine-grained integration of generic motif finders. *Bioinformatics* 24, 2288–2295. doi: 10.1093/bioinformatics/btn420

Yamashita, R., Wakaguri, H., Sugano, S., Suzuki, Y., and Nakai K. (2010). DBTSS provides a tissue specific dynamic view of Transcription Start Sites. *Nucleic Acids Res.* 38, D98–D104. doi: 10.1093/nar/gkp1017

Yamnik, R. L., and Holz, M. K. (2010). mTOR/S6K1 and MAPK/RSK signaling pathways coordinately regulate estrogen receptor a serine 167 phosphorylation. *FEBS Lett.* 584, 124–128. doi: 10.1016/j.febslet.2009.11.041

Yin, Y., She, H., Li, W., Yang, Q., Guo, S., and Mao, Z. (2012). Modulation of neuronal survival factor MEF2 by kinases in Parkinson's disease. *Front. Physiol.* 3:171. doi: 10.3389/fphys.2012.00171

Zambelli, F., Pesole, G., and Pavesi, G. (2009). Pscan: finding over-represented transcription factor binding site motifs in sequences from co-regulated or co-expressed genes. *Nucleic Acids Res.* 37, W247–W252. doi: 10.1093/nar/gkp464

Zambelli, F., Prazzoli, G. M., Pesole, G., and Pavesi, G. (2012). Cscan: finding common regulators of a set of genes by using a collection of genome-wide ChIP-seq datasets. *Nucleic Acids Res* 40, W510–W51. doi: 10.1093/nar/gks483

Zheng, C., Ren, Z., Wang, H., Zhang, W., Kalvakolanu, D. V., Tian, Z., et al. (2009). E2F1 Induces tumor cell survival via nuclear factor-kappa B-dependent induction of EGR1 transcription in prostate cancer cells. *Cancer Res.* 69, 2324–2331. doi: 10.1158/0008-5472.CAN-08-4113

Conflict of Interest Statement: The authors declare that the research was conducted in the absence of any commercial or financial relationships that could be construed as a potential conflict of interest.

Received: 01 April 2014; paper pending published: 13 April 2014; accepted: 09 May 2014; published online: 03 June 2014.

Citation: Jablonska A and Polouliakh N (2014) In silico discovery of novel transcription factors regulated by mTOR-pathway activities. Front. Cell Dev. Biol. 2:23. doi: 10.3389/fcell.2014.00023

This article was submitted to Systems Biology, a section of the journal Frontiers in Cell and Developmental Biology.

The Journal of Toxicological Sciences (J. Toxicol. Sci.)
Vol.38, No.4, 643-654, 2013

Original Article

Oral administration of pentachlorophenol induces interferon signaling mRNAs in C57BL/6 male mouse liver

Jun Kanno[1], Ken-ichi Aisaki[1], Katsuhide Igarashi[1], Satoshi Kitajima[1], Nae Matsuda[1], Koichi Morita[1], Masaki Tsuji[1], Noriko Moriyama[1], Yusuke Furukawa[1], Maki Otsuka[1], Erika Tachihara[1], Noriyuki Nakatsu[2] and Yukio Kodama[1]

[1]Division of Cellular and Molecular Toxicology, Biological Safety Research Center, National Institute of Health Sciences, 1-18-1 Kamiyoga, Setagaya-ku, Tokyo 158-8501, Japan
[2]Toxicogenomics Informatics Project, National Institute of Biomedical Innovation, 7-6-8 Asagi Saito Ibaraki-City, Osaka 567-0085, Japan

(Received June 17, 2013; Accepted June 25, 2013)

ABSTRACT — Pentachlorophenol (PCP) was monitored for transcriptome responses in adult mouse liver at 2, 4, 8 and 24 hr after a single oral administration at four dose levels, 0, 10, 30 and 100 mg/kg. The expression data obtained using Affymetrix GeneChip MOE430 2.0 were absolutized by the Percellome method and expressed as three dimensional (3D) surface graphs with axes of time, dose and copy numbers of mRNA per cell. We developed the programs RSort, for comprehensive screening of the 3D surface data and PercellomeExploror for cross-referencing and confirmed the significant responses by visual inspection. In the first 8 hr, approximately 100 probe sets (PSs) related to PXR/SXR and Cyp2a4 and other metabolic enzymes were induced whereas Fos and JunB were suppressed. At 24 hr, about 1,200 PSs were strongly induced. We cross-referenced the Percellome database consisting of 111 chemicals on the liver transcriptome and found that about half of the PSs belonged to the metabolic pathways including Nrf2-mediated oxidative stress response networks shared with some of the 111 chemicals. The other half of the induced genes were interferon signaling network genes (ISG) and their induction was unique to PCP. Toll like receptors and other pattern recognition receptors, interferon regulatory factors and interferon alpha itself were included but inflammatory cytokines were not induced. In summary, these data indicated that functional symptoms of PCP treatment, such as hyperthermia and profuse sweating might be mediated by the ISG rather than the previously documented mitochondrial uncoupling mechanism. PCP might become a hint for developing low molecular weight orally available interferon mimetic drugs following imiquimod and RO4948191 as agonists of toll-like receptor and interferon receptor.

Key words: Pentachlorophenol, Mouse, Liver, Interferon signaling genes, Percellome toxicogenomics

INTRODUCTION

The Percellome Toxicogenomics Project is designed to identify dynamic and extensive networks of genes whose time- and dose-dependent patterns of expression in response to a chemical allows its toxic effects to be predicted. For this project, we developed a standardization method for microarrays and quantitative PCR that produces copy number of mRNAs per one cell (designated as "Percellome method") (Kanno *et al.*, 2006). This method allowed us to directly and quantitatively compare gene expression data among samples, studies, organs and even species using four arithmetic operations. One hundred and eleven chemicals (as of June 2013, Supplementary Table 1), most of which are known for their toxicity, were examined using the standard protocol of the project.

Pentachlorophenol (PCP) was examined in adult male C57BL/6 mouse liver. This compound has been used for multiple purposes such as herbicide, insecticide, fungicide, disinfectant, and other preservative purposes, moreover, its metabolism and toxicity, including carcinogenicity have been well studied. PCP is known to induce morphological changes in liver, kidney, hematopoietic, respiratory, immune and neural systems together with irritation of exposed sites. Hepatocarcinogenicity was demonstrated in rodents; the postulated mechanism involves

Correspondence: Jun Kanno (E-mail: kanno@nihs.go.jp)

hydroxyl radical mediated DNA adduct formation and oxidative stress by the PCP metabolites. Functional symptoms, such as hyperthermia (sometimes life-threatening), profuse sweating, nausea, and uncoordinated movements were noted. Hyperthermia and other functional symptoms have been explained by the uncoupling of oxidative phosphorylation in mitochondria.

Here, we report that a comprehensive Percellome analysis revealed that PCP was the only chemical among the 111 tested in our project that strongly induced the interferon signaling gene (ISG) network. Additional pathways induced by PCP were Nrf2-mediated oxidative stress responses and other metabolic pathways more commonly seem among the 111 chemicals.

MATERIALS AND METHODS

Test chemical

PCP, standard grade (100.0% by gas chromatography coupled with flame ionization detector, Wako Pure Chemical Industries, Ltd., Tokyo, Japan) was dissolved in water containing 0.5% methyl cellulose (Shin-Etsu Chemical Co., Ltd., Tokyo, Japan).

Animal experiments

All experiments were carried out under approval of Experimental Animal Use Committee of National Institute of Health Sciences, Japan. C57BL/6 Cr Slc (Japan SLC, Inc., Shizuoka, Japan) twelve week-old male mice maintained in a barrier system with a 12 hr photoperiod were used in this study. Prior to the main study, a dose finding study was performed. This study revealed that 100 mg/kg was the maximum dose without clinical symptoms or alteration in H&E histology of the liver sampled 24 hr after single oral administration (a standard criteria for the top dose of the Percellome Project study). For the liver transcriptome experiments, forty eight mice were divided into four groups with twelve each, and given a single dose of PCP at 0, 10, 30 and 100 mg/kg by oral gavage. At 2, 4, 8 and 24 hr post-gavage, three randomly selected mice from each dose groups were euthanized by exsanguination under ether anesthesia and the livers were excised into ice-cooled plastic dishes. Tissue blocks weighing 30 to 60 mg were placed in an RNase-free 2 ml plastic tube (Eppendorf GmbH., Hamburg, Germany) and soaked in RNAlater (Ambion Inc., Austin, TX, USA) within 3 min of the beginning of anesthesia. The 12 animal sampling for each time point was finished within 25 to 30 min in order to avoid circadian-based variation within a time point.

Sample preparation and GeneChip measurement

The tissue blocks soaked in RNAlater were kept overnight at 4°C or until use. RNAlater was replaced in the 2 ml plastic tube with 1.0 ml of RLT buffer (Qiagen GmbH., Hilden, Germany), and the tissue was homogenized by adding a 5 mm diameter Zirconium bead (Funakoshi, Tokyo, Japan) and shaking with a MixerMill 300 (Qiagen GmbH) at a speed of 20Hz for 5 min (only the outermost row of the shaker box was used).

Three separate 10μl aliquots were taken from each sample homogenate to another tube and mixed thoroughly. A final 10 μl aliquot there from was treated with DNAse-free RNase A (Nippon Gene Inc., Tokyo, Japan) for 30 min at 37°C, followed by Proteinase K (Roche Diagnostics GmbH., Mannheim, Germany) for 3 hr at 55°C in 1.5 ml capped tubes. The aliquot was transferred to a 96-well black plate. PicoGreen fluorescent dye (Molecular Probes Inc., Eugene, OR, USA) was added to each well, shaken for 10 sec four times and then incubated for 2 min at 30°C. The DNA concentration was measured using a 96 well fluorescence plate reader with excitation at 485 nm and emission at 538 nm. λ phage DNA (PicoGreen Kit, Molecular Probes Inc.) was used as standard.

As reported previously, the graded-dose spike cocktail (GSC) made of the following five *Bacillus subtilis* RNA sequences were selected from the gene list of Affymetrix GeneChip arrays (AFFX-ThrX-3_at, AFFX-LysX-3_at, AFFX-PheX-3_at, AFFX-DapX-3_at, and AFFX-TrpnX-3_at) present in the MOE430 arrays was added to the sample homogenates in proportion to their DNA concentrations (Kanno *et al.*, 2006). Then, the sample homogenates spiked with GSC were processed according to the Affymetrix standard protocol. The GeneChips used were Mouse 430 2.0. We used the in house developed SCal4 (Spike Calculation version 4, by K.A.) to check the efficiency of *in vitro* transcription, and the dose-response linearity of the five GSC spikes and to produce Percellome data, i.e. absolutized mRNA copy numbers of each PS were generated.

The data consist of four dose levels and four time points, generating a 4 x 4 matrix. The mean value (m) with standard deviation (sd) was calculated from the triplicates for all of the probe sets (PSs) for each dose-time points. In order to better visualize the changes at 2 hr, the vehicle value was used for putative zero point, and drawn a 5 x 4 surface three-dimension (3D) surface graph with X-axis for dose, Y for time, and Z for expression as shown in Fig. 1.

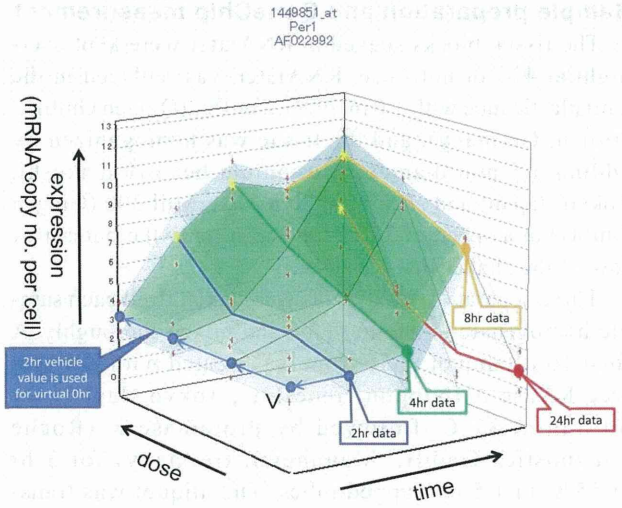

Fig. 1. Three dimensional surface expressions of Percellome Project data: The project data consist of four dose levels and four time points, generating 4 x 4 matrix. The mean value and standard deviation were calculated from the triplicate data. In order to better visualize the changes at 2 hr, the vehicle value was used for zero hour data to draw a 5 x 4 surface graph with X-axis for dose, Y for time, and Z for expression. Here, Affymetrix ID 1449851_at (Per1, period homolog 1) is shown. The 5 x 4 mesh made by the mean values was painted in translucent green (mean surface). The mean surface is rainbow-colored from blue, green, red to yellow according to its peak absolute values (cf. Fig. 3, Supplementary Fig. 1). Above and below the mean surface, +1sd and -1sd surfaces were overlaid using transparent blue. The dose-response curve at 2 hr, 4 hr, 8 hr and 24 hr are highlighted in blue, green, yellow and red. In a direction perpendicular to the dose-response curves, time course of each dose groups and vehicle group is indicated (not highlighted). The graph reads that the highest dose peaked at 4 hr at around 9 copies per cell; the middle dose peaked at 8 hr above 10 copies per cell. The vehicle group (V) showed the circadian change and peaked at 8 hr. The small red crosses are data of each animal sample (n = 3). Yellow asterisks indicate that the marked mean values were significantly different from concurrent vehicle value by $p < 0.05$ (Student's t-test).

Comprehensive selection of treatment-responding mRNAs

The in house developed software, RSort (Roughness Sort by K.A.) was used for automatic selection of treatment-responding mRNAs. This program sorts the PSs based on the roughness of the 3D surface. In other words, calculate the numbers of peaks (upward and downward) in a surface and sort by the number of peaks (maximum of eight peaks in 4 x 4 grid of the surface). Next, it filters the PSs by the number of peaks (normally three or less peaks) and additional parameters such as maximum expression level (normally more than one copy per cell for liver samples), p values between vehicle and top dose groups ($P < 0.05$ or $p < 0.01$). Here, a surface was selected when it had three peaks or less, the first peak in high doses (at any time) or the first peak in middle doses if its value is not significantly different from the neighboring high dose at $p < 0.01$ by Student's t-test, and the value of the peak is significantly different from that of vehicle control at $p < 0.05$ by Student's t-test. These automatically selected PSs were then visually checked for their 3D-surface shapes (to eliminate noisy data), and subdivided into those showed initial changes at 2, 4, 8, and 24 hr. A cross-referencing program named PE (Percellome Explorer, by K.A.) was used to select a list of chemicals that share PSs common to the visually confirmed list of PCP. The PE contains the gene lists automatically selected by the RSort of all data in our Percellome Project (168 datasets for liver samples, 286 for all samples), and automatically cross-refers and sorts out the chemicals sharing the same PSs (Fig. 2). The automatically selected gene lists (product sets) were visually checked to remove noise surfaces.

In Situ Hybridization

For *in situ* hybridization of Irf7 and Stat1 mRNAs, QuantiGeneViewRNA ISH Tissue Assay kit (Affymetrix, Inc., Santa Clara, CA, USA) was used. The probes were designed and synthesized by Affymetrix; regions covered were 2-1461 bases for Irf7 and 707-1710 bases for Stat1. 10% buffered formalin fixed liver tissues were dehydrated and embedded in paraffin. Tissue sections were mounted on "FRONTIER coated glass slides" (Matsunami Glass Ind., Ltd. Osaka, Japan). The slides were completely dried and stored until use. The slides were re-fixed in 10% formaldehyde for 1 hr at room temperature and washed with PBS and deparaffinized with xylene, pretreated in 1x Pretreatment Solution at 98°C for 30 min and digested with Protease QF at 40°C for 20 min. The probes were hybridized at 40°C for 2 hr and the signals were detected with Fast Red.

RESULTS

The numbers of PSs that started to change in response to PCP treatment at 2, 4, 8 and 24 hr were 98, 55, 127 and 1192 respectively (Supplementary Table 2, Supplementary Fig. 1). Chemicals or treatment in the Percellome database (Supplementary Table 1), that shared the PS list with PCP are shown in Table 1. The chemicals that shared the most with the 2 hr PS list of PCP

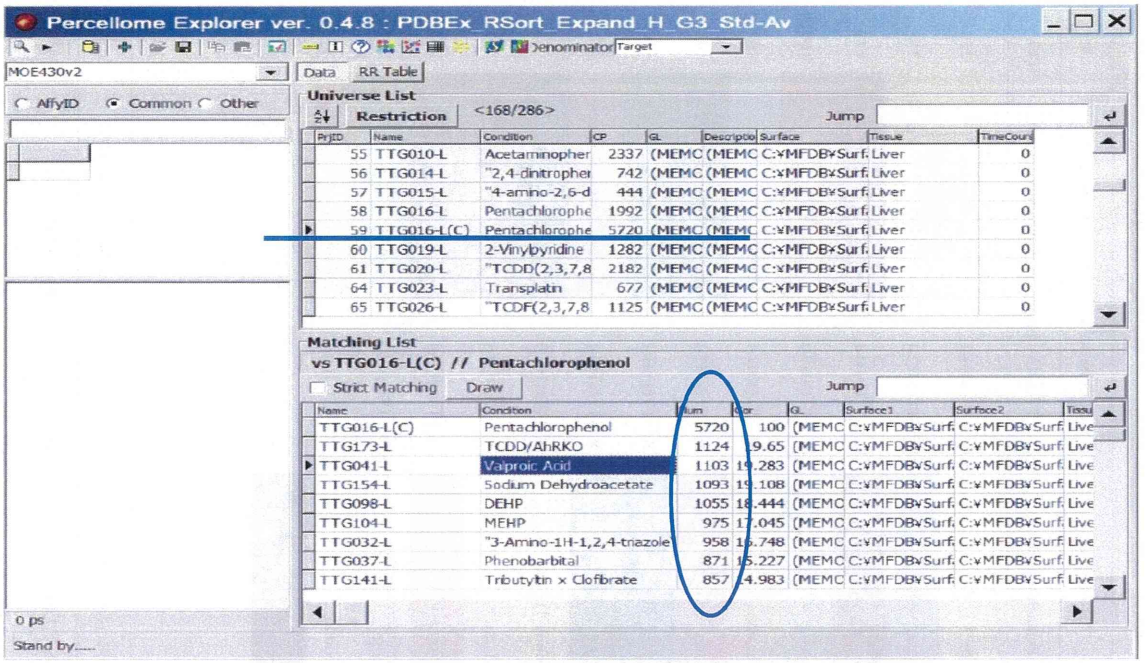

Fig. 2. PercellomeExplorer (PE) Software: The PE contains the gene lists automatically selected by the RSort software program of all data in our Percellome Project (168 datasets for liver samples, 286 for all samples, as of May 2013), and automatically picks up the chemicals sharing same PSs. TTG016-L(C), the study code for PCP was selected from the upper window and the chemicals sharing the PSs were listed in the lower window. These lists await visual confirmation.

was sodium dihydroacetate (TTG154-L); 51 PSs, followed by acephate (TTG109-L); 24 PSs, down to 5-fluorouracil (TTG160-L); 4 PSs. The sum set (or union of sets in set theory) of the 2 hr PS lists that are listed in the 2 hr column of the Table 1 contained 75 PSs (up-regulated (Up) 59, down-regulated (D) 16). Likewise, the sum set of the 4 hr PS lists contained 31 PSs (Up 22, D 9), 8 hr 46 PSs (Up 23, D 23) and 24 hr 636 PSs (all Up). The PS list unique to PCP (Unique list) at each time point contained 23, 24, 81, and 556 PSs at each time points (cf. Supplementary Table 2).

Profiles of genes changed at 2, 4 and 8 hr

The PS list common to other chemicals (Common list) contained the gluconeogenesis pathway of PGC-1A (Ppargc1a)/Foxo1/HNF4 (Puigserver *et al.*, 2003) that were induced at 2 hr (Fig. 3). This finding is in concordance with the report in experimental animals that PCP acutely induces hyperglycemia (Deichman *et al.*, 1942; Clayton and Clayton, 1981). Ppargc1a was reported to increase the expression of Lpin1 (Finck *et al.*, 2006), which was also the case here. A small set of genes encoding metabolic enzymes was induced during the first 8 hr, including Cyp2a4, Cyp4f16, Cyp7a1, Cyp17a1, Cyp39a1, Fmo2, and Fmo5 (Fig. 3).

Ingenuity pathway analysis (Ingenuity Systems, Inc. Redwood City, CA, USA) indicated that these genes are likely to be induced by Nr1i3 (CAR), Nr1i2 (PXR/SXR) or Nr5a1 (data not shown). Although our RSort program did not identify these nuclear receptors, manual search showed that PXR/SXR was induced by PCP (Fig. 3). These changes were not unique to PCP and shared by some of the chemicals in the Common list (cf. Supplementary Table 2).

Down regulation of Fos and JunB at 2, 4, and 8 hr (Fig. 3) was uniquely found in the PCP gene list. Bioinformatic analysis did not identify any associated pathways.

Profiles of genes started to change at 24 hr

The list of PSs induced at 24 hr contained two large networks. About half of the PSs showing altered expression by PCP were assigned to the interferon signaling pathway (Fig. 4, Supplementary Fig. 1). The interferon signaling genes (ISG) were highly up-regulated from Stat1, Stat2, Tyk, to Irf7, Myd88, Oas, Ifit, Cxcl10 and other downstream targets. Toll like receptors (TLRs) and

Table 1. The total numbers of probesets induced by PCP at each time points and those shared with other chemicals.

2 hr			4 hr			8 hr			24 hr		
Percellome No.	Treatment	PS	Percellome No.	Treatment	PS	Percellome No.	Treatment	PS	Percellome No.	Treatment	PS
TTG016-L(C)	Pentachlorophenol	98	TTG016-L(C)	Pentachlorophenol	55	TTG016-L(C)	Pentachlorophenol	127	TTG016-L(C)	Pentachlorophenol	1192
TTG154-L	Sodium Dehydroacetate	51	TTG104-L	MEHP	21	TTG098-L	DEHP	15	TTG098-L	DEHP	258
TTG109-L	Acephate	24	TTG098-L	DEHP	16	TTG041-L	Valproic Acid	14	TTG032-L	3-Amino-1H-1,2,4-triazole	212
TTG059-L	Caffeine	19	TTG037-L	Phenobarbital	14	TTG104-L	MEHP	14	TTG104-L	MEHP	177
TTG062-L(C)	Dexamethasone	18	TTG032-L	3-Amino-1H-1,2,4-triazole	12	TTG109-L	Acephate	13	TTG037-L	Phenobarbital	160
TTG041-L	Valproic Acid	18	TTG144-L	Tributyltin x Phenobarbital	12	TTG160-L	5-fluorouracil	10	TTG041-L	Valproic Acid	109
TTG098-L	DEHP	17	TTG150-L	Valproic acid sodium salt x Thalidomide	8	TTG154-L	Sodium Dehydroacetate	9	TTG157-L	Valproic acid sodium salt	103
TTG019-L	2-Vinylpyridine	15	TTG141-L	Tributyltin x Clofibrate	8	TTG141-L	Tributyltin x Clofibrate	8	TTG031-L	2-Chloro-4,6-dimethylaniline	94
TTG104-L	MEHP	12	TTG074-L	Bromobenzene	8	TTG031-L	2-Chloro-4,6-dimethylaniline	8	TTG154-L	Sodium Dehydroacetate	77
TTG165-L	Chlorpyrifos	12	TTG151-L	Valproic acid sodium salt x Valproic acid sodium salt	7	TTG032-L	3-Amino-1H-1,2,4-triazole	8	TTG162-L	Sesame seed oil unsaponified matter	71
TTG034-L	4-Ethylnitrobenzene	12	TTG031-L	2-Chloro-4,6-dimethylaniline	7	TTG146-L	Forskolin	6	TTG044-L	Clofibrate	69
TTG166-L	Carbaryl	10	TTG044-L	Clofibrate	6	TTG062-L(C)	Dexamethasone	6	TTG074-L	Bromobenzene	47
TTG031-L	2-Chloro-4,6-dimethylaniline	10	TTG162-L	Sesame seed oil unsaponified matter	5	TTG054-L	Diethylnitrosamine (C57BL/6)	5	TTG109-L	Acephate	17
TTG141-L	Tributyltin x Clofibrate	9				TTG132-L	Curcumin	3	TTG160-L	5-fluorouracil	13
TTG032-L	3-Amino-1H-1,2,4-triazole	9				TTG136-L	Phytol	2			
TTG027-L	1,2,3-Triazole	9									
TTG160-L	5-fluorouracil	4									
	Sum Set (common)	75		Sum Set (common)	31		Sum Set (common)	46		Sum Set (common)	636
	Sum Set (Up)	59		Sum Set (Up)	22		Sum Set (Up)	23		Sum Set (Up)	636
	Sum Set (Dn)	16		Sum Set (Dn)	9		Sum Set (Dn)	23		Sum Set (Dn)	0
	PCP NOT Sum (unique to PCP)	23		PCP NOT Sum (unique to PCP)	24		PCP NOT Sum (unique to PCP)	81		PCP NOT Sum (unique to PCP)	556

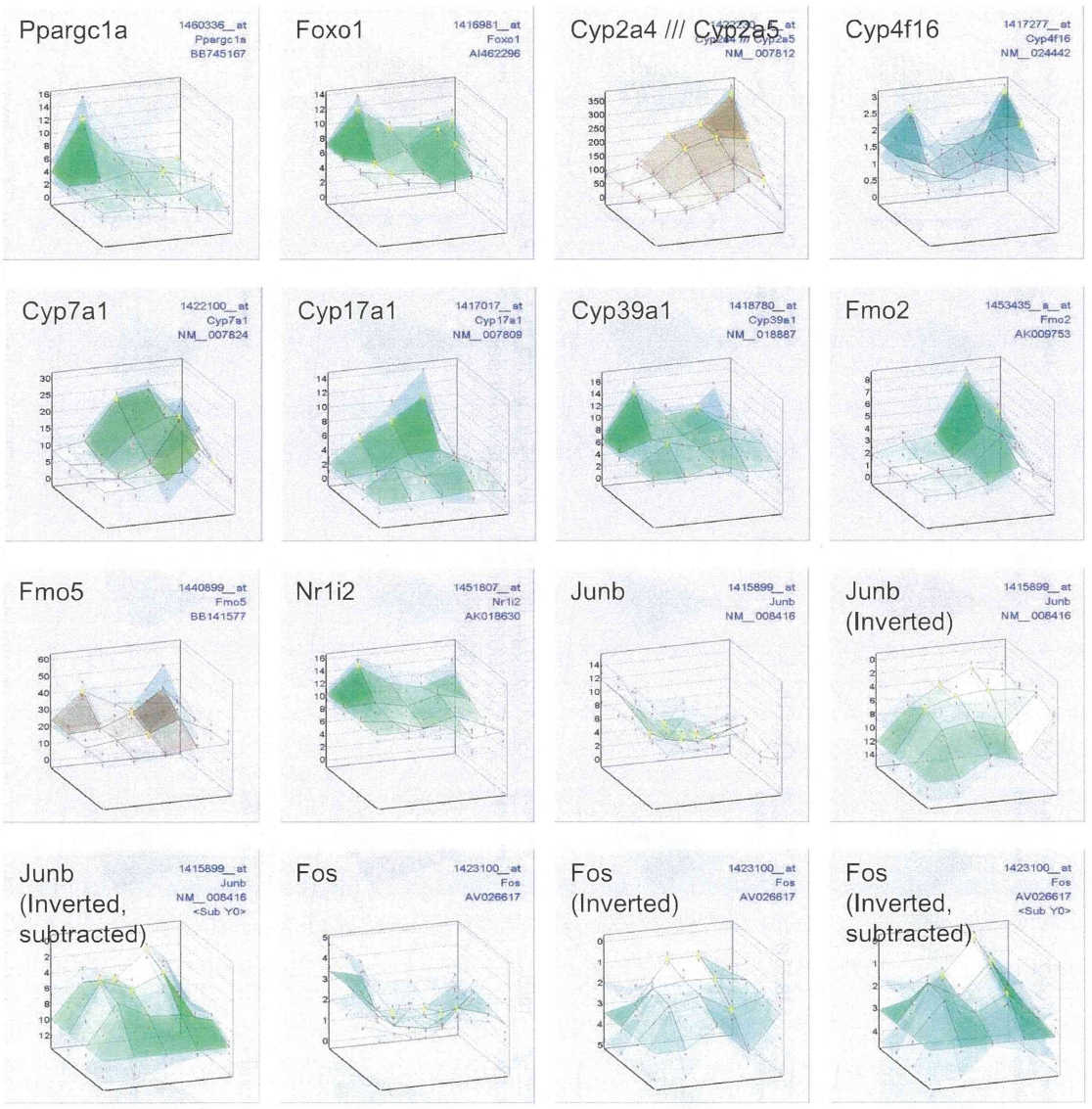

Fig. 3. Representative surface data of PSs induced at 2, 4 and 8 hr after PCP single gavage: Ppargc1a and Foxo1 are the members of gluconeogenesis pathway. A small set of genes of metabolic enzymes, such as Cyp2a4, Cyp4f16, Cyp7a1, Cyp17a1, Cyp39a1, Fmo2, and Fmo5 are induced during the first 8 hr. Nr1i2 or PXR/SXR is also induced. Down regulation of JunB and Fos at 2, 4, and 8 hr are noted. The graphs marked with (Inverted) are plotted with inverted z-axis, zero on top for better indication of suppression. The graphs with (Inverted, subtracted) are plotted, in addition to inverted z-axis, with the 2, 4, 8 and 24 hr values compensated by concurrent vehicle values so that the vehicle line is straight and cancels out the circadian changes.

other pattern recognition receptors (PRR), interferon regulatory factors (Irf) and interferon (Ifn) itself were included. These ISGs were uniquely induced by PCP. It is notable that inflammatory cytokines such as Tnf-α, IL-12 and CD40 were not effectively induced by PCP. The Ingenuity Pathways also plotted many genes in the interferon signaling with a very high probability score (Fig. 6).

In situ hybridization confirmed that hepatocytes were producing the Irf7 and Stat1 in a dose dependent manner (Fig. 7, only vehicle and top dose were shown).

The other half was assigned, by Ingeunity Pathway analysis, to Nrf2-mediated Oxidative Stress Responses